JVI Journals.ASM.org

# Identification of the Receptor-Binding Domain of the Spike Glycoprotein of Human Betacoronavirus HKU1

Zhaohui Qian,[a,b] Xiuyuan Ou,[a] Luiz Gustavo Bentim Góes,[b]* Christina Osborne,[b] Anna Castano,[c] Kathryn V. Holmes,[c] Samuel R. Dominguez[b]

MOH Key Laboratory, Institute of Pathogen Biology, Chinese Academy of Medical Science, Beijing, China[a]; Departments of Pediatrics[b] and Microbiology,[c] University of Colorado School of Medicine, Aurora, Colorado, USA

## ABSTRACT

**Coronavirus spike (S) glycoproteins mediate receptor binding, membrane fusion, and virus entry and determine host range. Murine betacoronavirus (β-CoV) in group A uses the N-terminal domain (NTD) of S protein to bind to its receptor, whereas the β-CoVs severe acute respiratory syndrome CoV in group B and Middle East respiratory syndrome CoV in group C and several α-CoVs use the downstream C domain in their S proteins to recognize their receptor proteins. To identify the receptor-binding domain in the spike of human β-CoV HKU1 in group A, we generated and mapped a panel of monoclonal antibodies (MAbs) to the ectodomain of HKU1 spike protein. They did not cross-react with S proteins of any other CoV tested. Most of the HKU1 spike MAbs recognized epitopes in the C domain between amino acids 535 and 673, indicating that this region is immunodominant. Two of the MAbs blocked HKU1 virus infection of primary human tracheal-bronchial epithelial (HTBE) cells. Preincubation of HTBE cells with a truncated HKU1 S protein that includes the C domain blocked infection with HKU1 virus, but preincubation of cells with truncated S protein containing only the NTD did not block infection. These data suggest that the receptor-binding domain (RBD) of HKU1 spike protein is located in the C domain, where the spike proteins of α-CoVs and β-CoVs in groups B and C bind to their specific receptor proteins. Thus, two β-CoVs in group A, HKU1 and murine CoV, have evolved to use different regions of their spike glycoproteins to recognize their respective receptor proteins.**

## IMPORTANCE

**Mouse hepatitis virus, a β-CoV in group A, uses the galectin-like NTD in its spike protein to bind its receptor protein, while HCoV-OC43, another β-CoV in group A, uses the NTD to bind to its sialic-acid containing receptor. In marked contrast, the NTD of the spike glycoprotein of human respiratory β-CoV HKU1, which is also in group A, does not bind sugar. In this study, we showed that for the spike protein of HKU1, the purified C domain, downstream of the NTD, could block HKU1 virus infection of human respiratory epithelial cells, and that several monoclonal antibodies that mapped to the C domain neutralized virus infectivity. Thus, the receptor-binding domain of HKU1 spike glycoprotein is located in the C domain. Surprisingly, two β-CoVs in group A, mouse hepatitis virus and HKU1, have evolved to use different regions of their spike glycoproteins to recognize their respective receptors.**

Coronaviruses (CoVs) primarily cause respiratory and enteric diseases in humans, animals, and birds, and some CoVs also cause systemic diseases, including hepatitis or neurological diseases (1). Since the 2002-2003 epidemic of severe acute respiratory syndrome (SARS), intensive surveillance of humans and animals has led to the discovery of numerous other CoVs (2, 3). Phylogenetically, CoVs now are divided into four genera, called the α-, β-, γ-, and δ-CoVs (4). Currently there are six CoVs known to infect humans: two α-CoVs, 229E and NL63; two β-CoVs in group A, OC43 and HKU1; one β-CoV in group B, SARS-CoV; and one β-CoV in group C, Middle East respiratory syndrome coronavirus (MERS-CoV), that currently is causing an epidemic with an ~30% fatality rate (5–12). While the first four of these human CoVs circulate only in humans and predominately cause mild respiratory diseases, SARS-CoV and MERS-CoV are zoonoses associated with episodically emerging epidemics of severe respiratory infection, including pneumonia, the acute respiratory distress syndrome (ARDS), and death in about 10% to 30% of cases (12, 13).

The large spikes on the envelope of CoV virions consist of trimers of the ~200-kDa spike (S) glycoprotein that bind to host-specific receptors; mediate virus entry, tissue tropism, and host range; and can affect virus virulence. S protein is the target for CoV neutralizing antibodies and is an essential component of CoV vaccines and vaccine candidates. CoV S proteins are class I viral fusion proteins, like influenza virus hemagglutinin (HA), HIV Env, Ebola virus G, and paramyxovirus F glycoproteins (14). CoV S proteins contain two subunits, called S1 and S2, which are

**Received** 31 December 2014 **Accepted** 4 June 2015

**Accepted manuscript posted online** 17 June 2015

**Citation** Qian Z, Ou X, Góes LGB, Osborne C, Castano A, Holmes KV, Dominguez SR. 2015. Identification of the receptor-binding domain of the spike glycoprotein of human betacoronavirus HKU1. J Virol 89:8816–8827. doi:10.1128/JVI.03737-14.

**Editor:** S. Perlman

Address correspondence to Zhaohui Qian, zqian2013@sina.com, or Samuel R. Dominguez, Samuel.dominguez@ucdenver.edu.

Z.Q. and X.O. contributed equally to this study.

* Present address: Luiz Gustavo Bentim Góes, Laboratório de Virologia Clínica e Molecular, Departamento de Microbiologia, Instituto de Ciências Biomédicas, Universidade de São Paulo, São Paulo, Brazil.



doi:10.1128/JVI.03737-14

separated by a protease-sensitive amino acid sequence. S1 determines the specificity of receptor binding, while S2 mediates membrane fusion and virus entry. Specific host membrane proteins have been identified as receptors for the S1 domains of various α- and β-CoVs, and host-specific differences in a particular CoV receptor protein can determine the viral host range (15–25). CoV S1 proteins generally contain two important domains. The first is the N-terminal domain (NTD) that contains the receptor-binding site for murine β-CoV mouse hepatitis virus (MHV) in group A (19) and also binds to sialic acid-containing moieties on host cell membranes for several α-CoVs, such as transmissible gastroenteritis coronavirus (TGEV) of swine (26), several β-CoVs in group A, such as HCoV-OC43 and bovine CoV (27), avian γ-CoV, and infectious bronchitis virus (IBV) (28). The second domain in S1 is the C domain that lies downstream of the NTD and contains a variety of receptor-binding motifs that recognize host-specific determinants of aminopeptidase N (APN), angiotensin converting enzyme 2 (ACE2), or dipeptidyl peptidase 4 (DPP4) proteins that act as receptors for different CoVs (29). Identification of the receptor for a CoV and characterization of the domain of the viral S1 protein that binds to specific sites on its receptor can aid in development of vaccines, elucidate how the CoV jumps from one host to another, and help to elucidate the complex changes in the spike glycoproteins during CoV evolution.

Human β-CoV HKU1 virus in group A first was discovered in Hong Kong in 2004 (11) and subsequently has been found in humans worldwide, where it accounts for about 0.9% (0 to 4.3%) of acute respiratory infections (30, 31). It is estimated that the majority of children have been exposed to HKU1 before age 6 (32). Although HKU1 infections generally result in mild upper respiratory tract disease, occasionally HKU1 can cause severe respiratory diseases, including pneumonia in very young children, the elderly, and immunocompromised patients (33). Biological studies of HKU1 were challenging initially because infectious virus could not be readily isolated from clinical specimens in continuous cell lines. The recent discoveries that HKU1 can be isolated in primary, differentiated human tracheal bronchial epithelial (HTBE) cells and human alveolar type II (ATII) cells cultured at an air-liquid interface has expedited isolation and characterization of this ubiquitous human CoV from human clinical specimens (34–37). In this study, we used our newly generated HKU1 S protein-specific neutralization antibodies and N-terminal or C-terminal truncated S1 proteins to determine the location of the RBD of the HKU1 S protein.

## MATERIALS AND METHODS

**Cell lines.** Vero E6 (African green monkey kidney epithelial cell line), MRC5 (human fetal lung fibroblast), HRT18 (human rectal tumor cell line), MDCK (Madin-Darby canine kidney cell line), and 293T (human embryonic kidney 293 cell line transformed with simian virus 40 [SV40] large T antigen) were obtained from the ATCC (Manassas, VA). All of these cell lines were maintained in Dulbecco's modified Eagle's medium (DMEM) with 10% fetal bovine serum (FBS) and 2% penicillin, streptomycin, and fungizone (PSF) (Life Technologies Inc.). The LLCMK2 cell line, kindly provided by Lia Van der Hoek (Academic Medical Center of the University of Amsterdam), was maintained in Opti-MEM1 with 10% FBS and 2% PSF. Primary human tracheal/bronchial epithelial (HTBE) cells were obtained from LifeLine Cell Technology (Frederick, MD) and cultured and differentiated as previously reported (35). Briefly, HTBE cells were grown in BronchiaLife complete medium (BronchiaLife basal medium with BronchiaLife B/T LifeFactors; LifeLine Cell Technology, Frederick, MD) and plated on 12-well Corning transwells (collagen-coated and permeable; 0.4 μm; St. Louis, MO) until confluence and then switched to differentiation medium as previously described (35). Prior to virus inoculation, HTBE cell cultures were maintained for 3 weeks in differentiation media at an air-liquid interface to generate well-differentiated, polarized cultures that resembled *in vivo* ciliated respiratory epithelium.

**Viruses.** Isolation and propagation of HKU1 virus (number 21) in HTBE cells have been described elsewhere (35, 37). Briefly, differentiated HBTE cells at the air-liquid interface were inoculated on the apical surface with 150 μl per insert of each clinical sample (primary isolate) diluted 1:10 in DMEM containing 1% bovine serum albumin fraction V (BSA) or with a 1:10 or 1:100 dilution of passage 1 (P1) virus stock generated from apical washes of primary cultures from HBTE cells harvested at 48 or 72 h postinoculation (hpi). After 4 h of incubation at 34°C, the virus inocula were removed, and the HBTE cells were maintained at an air-liquid interface. Amplified viruses were harvested at 48 or 72 h postinoculation by rinsing apical surfaces twice with 150 μl of DMEM plus 1% BSA. Human coronaviruses 229E and NL63, bovine coronavirus (BCoV) Mebus strain, and MHV A59 were propagated in MRC5, LLCMK2, HRT18, and 17Cl.1 cells, respectively. The Urbani strain of SARS-CoV was kindly provided by W. J. Bellini at the Centers for Disease Control and Prevention (Atlanta, GA) and was propagated in Vero E6 cells. All work with infectious SARS-CoV was performed in the biosafety level 3 laboratory at the University of Colorado School of Medicine (Aurora, CO).

**Constructs and plasmids.** The full-length, codon-optimized genotype A HKU1 spike gene preceded by a Kozak sequence was synthesized by GenScript (Piscataway, NJ) and cloned into pcDNA3.1(+) (Invitrogen) between HindIII and XbaI sites for eukaryotic expression. To eliminate a furin cleavage site and minimize cleavage between S1 and S2, both arginine 759 and arginine 760 were mutated with alanine substitutions in the HKU1 $S_{aa}$ construct. HKU1 $S_{aa}$ served as the template to make a C-terminally truncated construct, HKU1-$S_{ecto}$ (see Fig. 4), which expresses the soluble ectodomain (amino acids [aa] 1 to 1283) with a linker (GGGGS) and a C-terminal FLAG tag. A series of deletion constructs encoding HKU1 S14-755, S14-673, S14-534, S14-443, S14-294, S295-755, and S295-673 were amplified using the following primer pairs: S14-755 Fwd, ATCGCTAGCCGTCATAGGCGACTTCAACTG; Rev, ATCGGATCCG AACTTGAACTTGATGATGGTGAG; S14-673 Fwd, ATCGCTAGCCGT CATAGGCGACTTCAACTG; Rev, ATCGGATCCGATGGAAATATATT GTATGTCTTGTTG; S14-534 Fwd, ATCGCTAGCCGTCATAGGCGAC TTCAACTG; Rev, ATCGGATCCGATGTTTTGCACTGTATTTCACTA AAG; S14-443 Fwd, ATCGCTAGCCGTCATAGGCGACTTCAACTG; Rev, ATCGGATCCGAAGAAGAAGGATTATAGTTG; S14-293 Fwd, AT CGCTAGCCGTCATAGGCGACTTCAACTG; Rev, ATCGGATCCGAG CTGCAAGATCTGGGATCGTAG; S295-755 Fwd, ATCGCTAGCCAAA TCCCTCCTTCCCAATACTG; Rev, ATCGGATCCGAACTTGAACTTG ATGATGGTGAG; S310-673 Fwd, ATCGCTAGCCGTTAAGCCTGTGG CTACGGTG; Rev, ATCGGATCCGATGGAAATATATTGTATGTCTTG TTG. HKU1 $S_{aa}$ was used as a template. The PCR products then were inserted between NheI and BamHI sites of pIg (a kind gift of Michael Farzan, Scripps Research Institute, Florida campus), which provides a CD5 signal peptide before NheI and human Fc tag after BamHI (38). Constructions of plasmids encoding trimeric, plasma membrane-bound SARS SΔ19 and MERS SΔ16 glycoproteins are described elsewhere (39, 40).

**Protein expression and purification of HKU1 spike glycoprotein.** To express the soluble HKU1-$S_{ecto}$ and truncated HKU1 S glycoproteins, plasmids (50 μg per T150 flask) were transfected into HEK 293T cells at 70 to 80% confluence using polyethylenimine (Polyscience Inc., Warrington, PA). After 16 h, cells were washed once and refed with 293 serum-free medium (HyClone, Logan, UT). Supernatants containing $S_{ecto}$ and truncated S proteins were harvested at 40 h and 64 h posttransfection. Soluble S proteins were purified by affinity chromatography using either an anti-FLAG M2 bead column for HKU1-$S_{ecto}$ or a protein G column for

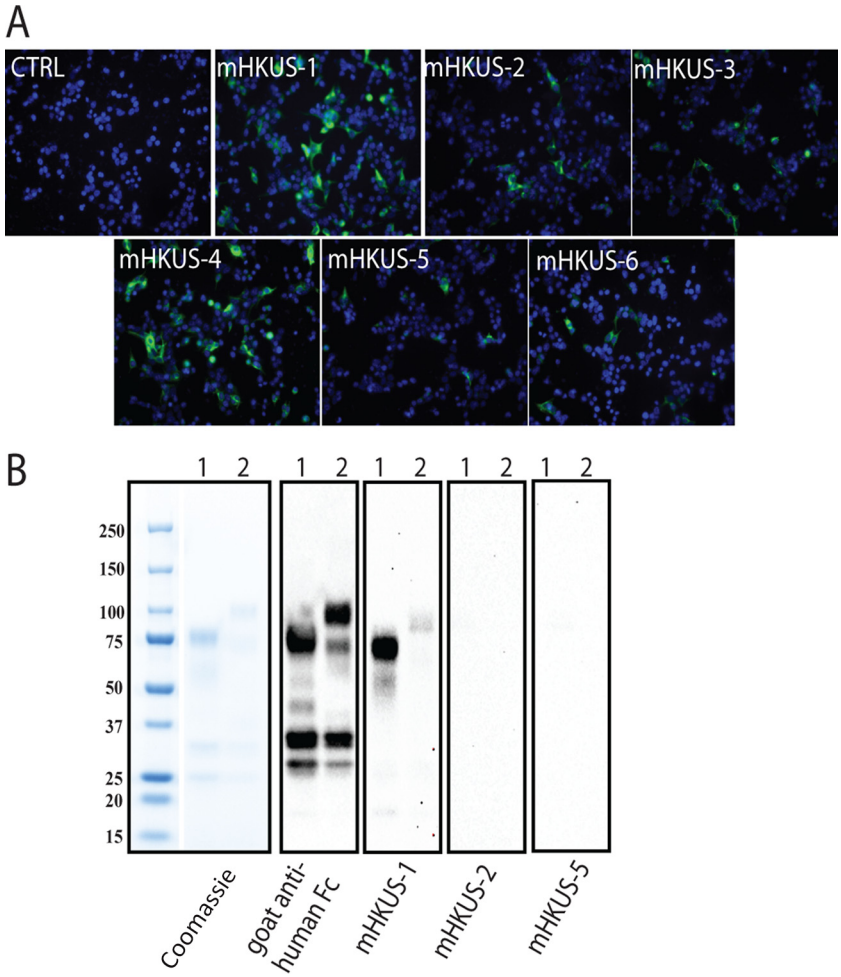


**FIG 1** Binding of mouse monoclonal antibodies to HKU1 S. (A) IFA. HEK 293T cells expressing HKU1 S protein were fixed and stained with the indicated MAbs (undiluted hybridoma supernatants), followed by FITC-conjugated goat anti-mouse IgG. The concentration of antibody in each undiluted hybridoma supernatant was the following: mHKUS-1, 25 μg/ml; mHKUS-2, 6.0 μg/ml; mHKUS-3, 4.0 μg/ml; mHKUS-4, 12.4 μg/ml; mHKUS-5, 25 μg/ml; mHKUS-6, 6.8 μg/ml. The experiment was repeated at least 3 times. CTRL, control. (B) Western blot analysis. Lane 1, 1 μg of purified Fc-tagged S14-294aa protein; lane 2, 1 μg of purified Fc-tagged S295-755aa protein. The blots were probed with either HRP-conjugated goat anti-human IgG or the indicated MAbs (undiluted hybridoma supernatants), followed by HRP-conjugated goat anti-mouse IgG. The experiments were done twice.

Fc-tagged truncated proteins, and the purified S proteins were detected by Western blotting with either anti-FLAG M2 or anti-Fc antibody. The purity of each protein preparation was demonstrated by SDS-PAGE followed by Coomassie staining, and the concentration of each protein was calculated according to the following equation: protein concentration = (OD value of the protein measured by Nanodrop at 280 nm)/(protein extinction coefficient), where the coefficients were the following: (S1-Fc, 1.67; NTD-Fc, 1.62; C domain-Fc, 1.44).

**Generation of monoclonal antibodies to HKU1-$S_{ecto}$ protein.** Eight- to 10-week-old BALB/c mice were immunized with 100 μg of HKU1-$S_{ecto}$ protein with 100 μl of TiterMax gold adjuvant (Sigma-Aldrich, St. Louis, MO) at days 0, 14, 28, and 42. Injections were alternated between subcutaneous and intraperitoneal routes, and the final injection was done with HKU1-$S_{ecto}$ proteins with PBS instead of adjuvant. Three days after the final boost, mice were euthanized, spleens were harvested, and splenocytes were fused with myeloma cells to generate hybridomas that were cloned. The supernatant medium of each hybridoma clone was screened for the presence of antibody. Antibodies to HKU1 spike protein were detected by enzyme-linked immunosorbent assay (ELISA), Western blotting, and immunofluorescence assay (IFA).

**Generation of rabbit polyclonal antibodies to HKU1-$S_{ecto}$ protein.** Two rabbits (1811 and 1814) were prescreened as negative for the presence of cross-reactive antibodies to the HKU1 spike glycoprotein in their sera and were immunized with 100 μg of purified HKU1-$S_{ecto}$ protein with Freud's complete adjuvant, followed by boosters at days 14, 42, and 56 (Open Biosystems, Huntsville, AL). Two weeks following the final booster, sera were collected and total IgG was purified using a protein G column. Antibodies to HKU1 spike protein were detected by ELISA, Western blotting, and IFA.

**ELISA.** Immulon 2HB plates (Thermo, Rochester, NY) were coated overnight with 0.5 μg per well of goat anti-human IgG. After blocking with 3% BSA, plates were incubated overnight at 4°C with either purified truncated, Fc-tagged HKU1 S proteins or 100 μl of culture supernatants containing truncated, Fc-tagged HKU1 S proteins. After washing, hybridoma supernatants containing MAbs or purified antibodies serially diluted in PBS with 3% BSA were added to the wells and incubated at room temperature (RT) for 1 h. Unbound MAb was removed by washing, and MAb bound to the truncated, Fc-tagged S proteins was detected by horseradish peroxidase-conjugated goat anti-mouse Ig (Jackson ImmunoResearch, West Grove, PA) diluted 1:1,000 and incubated at room temperature for 1 h. After washing, 100 μl of *o*-phenylenediamine dihydrochloride (OPD) (Sigma, St. Louis, MO) was added to each well and incubated for 15 min. The reaction then was stopped by addition of 2 M sulfuric acid. The optical density was

**TABLE 1** Summary of IFA, Western blotting, ELISA, and HKU1 virus neutralization studies of mouse monoclonal antibodies to HKU1 S glycoprotein

| Antibody and assay | mHKUS-1 | mHKUS-2 | mHKUS-3 | mHKUS-4 | mHKUS-5 | mHKUS-6 |
|---|---|---|---|---|---|---|
| IFA[a] | | | | | | |
| HKU1 S | ++++ | + | ++ | ++++ | + | + |
| SARS S and infection | − | − | − | − | − | − |
| MHV S and infection | − | − | − | − | − | − |
| MERS S | − | − | − | − | − | − |
| BCoV infection | − | − | − | − | − | − |
| 229E infection | − | − | − | − | − | − |
| NL63 infection | − | − | − | − | − | − |
| Western[b] | | | | | | |
| S14-294aa | ++++ | − | − | − | − | − |
| S295-755aa | + | − | − | − | − | − |
| ELISA[c] | | | | | | |
| HKU1 Secto | ++++ | ++++ | ++++ | ++++ | ++++ | ++++ |
| S14-755aa | ++++ | ++++ | ++++ | ++++ | ++++ | ++++ |
| S14-673aa | ++++ | ++++ | ++++ | ++++ | ++++ | ++++ |
| S14-534aa | ++++ | − | − | − | − | − |
| S14-443aa | ++++ | − | − | − | − | − |
| S14-294aa | ++++ | − | − | − | − | − |
| S295-755aa | + | ++++ | ++++ | ++++ | ++++ | ++++ |
| S295-673aa | + | ++++ | ++++ | ++++ | ++++ | ++++ |
| Neutralization[d] | − | ++++ | ++++ | − | − | − |

[a] For IFA, ++++ indicates that the percentage of virus antigen-positive cells was equal to or greater than 20%; +++, between 10 and 20%; ++, between 5 and 10%; +, between 1 and 5%; −, no positive cells. For HKU1 S, MHV S, SARS S, and MERS S infection, cells were transduced with plasmids encoding the membrane-anchored S proteins of these viruses. For SARS, MHV, BCoV, 229E, and NL63 infection, cells expressing the appropriate virus receptor proteins were infected with the indicated virus.
[b] For Western blotting, ++++ indicates very strong signal; +++, strong signal; ++, weak signal; +, very weak signal; −, no signal.
[c] For ELISA, ++++ indicates positive signal at 1:4,096 dilution of MAb or further; +++, positive signal at dilution between 1:256 and 1:4,096; ++, positive signal at dilution between 1:4 and 1:256; +, positive signal from undiluted or 1:4 dilution of hybridoma supernatant; −, no signal with undiluted hybridoma supernatant.
[d] For neutralization, ++++ indicates greater than 100-fold inhibition of HKU1 virus infection, corresponding to the amount of viral RNA detected by real-time PCR in released virus at 48 hpi; +++, 10- to 100-fold inhibition; ++, 5- to 10-fold inhibition; +, 2- to 5-fold inhibition; −, no inhibition.

read on a BioTek Synergy HT plate reader (BioTek, Winooski, VT) at 492 nm.

**IFA.** The specificity of the MAbs was determined by IFA on cell cultures that displayed spike proteins of various CoVs on their plasma membranes. Cells transfected with plasmids encoding the spike glycoproteins of CoVs MHV, NL63, SARS, MERS, or HKU1 or cells infected with CoVs MHV, NL63, SARS, BCoV, 229E, or HKU1 were washed twice with DMEM or PBS and then fixed in 100% methanol for 20 min at −20°C. As positive controls for expression of the CoV S proteins on the fixed cells, the following antisera were used. MHV S protein was detected with polyclonal goat anti-MHV S antibody AO4 at a 1:200 dilution; 229E and NL63 S proteins were detected with mouse monoclonal anti-NL63 S protein antibody 165 (kind gift from Donna Ambrusino, MassBiologics, Boston, MA) at 10 μg/ml; SARS S protein was detected using rabbit anti-SARS S antibody IMG 636 (Novus, Littleton, CO) at 1:200 dilution; MERS S protein was detected using mouse monoclonal anti-FLAG M2 (Sigma, St. Louis, MO) at 1:200 dilution; BCoV infection was detected using mouse monoclonal antibody to MHV nucleocapsid protein (a kind gift from J. Liebowitz, Texas A&M College of Medicine, Bryan, TX) at 10 μg/ml; and HKU1 S protein was detected using rabbit 1814 polyclonal antibody to HKU1 S protein at a 1:100 dilution. Bound antiviral antibodies were visualized using the following fluorescein isothiocyanate (FITC)-conjugated secondary antibodies: rabbit anti-goat IgG, goat anti-mouse IgG, or goat anti-rabbit IgG (Jackson ImmunoResearch, West Grove, PA) at 1:200 dilutions. Immunolabeled cells were imaged using a Zeiss Axioplan 2 or Nikon Eclipse TE2000-U fluorescence microscope.

**Real-time PCR.** Real-time PCR was performed as previously described by Kuypers et al. (41) using RNA ultrasense one-step quantitative reverse transcription-PCR (qRT-PCR) from Invitrogen, with minor modifications (36). Briefly, viral RNA was extracted from 140 μl of virus-containing apical wash using a BioRobot from Qiagen, and 10 μl of viral RNA extract was mixed with 10 μl of master mix containing 0.8 μl of $H_2O$, 1 μl of enzyme, 4 μl of 5× buffer, 0.2 μl of 10 μM probe (ATAATCCCA ACCCATRAG), 1 μl of 10 μM primer F1 (TGGTGGCTGGGACGATAT GT), 2.5 μl of 10 μM each primer mix (F2, TTTATGGTGGTTGGAATA ATATGTTG; F3, TGGCGGGTGGGATAATATGT; R1, GGCATAGCAC GATCACACTTAGG; R2, GGCAAAGCTCTATCACATTTGG; and R3, GAGGGCATAGCTCTATCACACTTAGG), and 0.5 μl of $MgSO_4$. RT-PCR was performed using a Roche LightCycler 480 under the following conditions: 50°C for 15 min, followed by 95°C for 2 min and then 45 cycles of 95°C for 15 s and 60°C for 30 s. To calculate the viral genome copy number in the samples, serially diluted synthetic DNA fragment containing the sequence of positions 15348 to 15442 of the HKU1 genome was used as the quantitative standard for real-time PCR.

**Western blotting.** Spike proteins on virions released into the supernatant media over infected cells or purified spike proteins were analyzed on 4 to 15% SDS-acrylamide gels and transferred to nitrocellulose membranes. The blot was blocked with 5% nonfat milk for 1 h at room temperature, and proteins were detected directly either with horseradish peroxidase (HRP)-conjugated goat anti-human IgG (Abcam, Cambridge, MA) at a 1:2,500 dilution or with supernatant media over hybridomas cloned from mice immunized with HKU1 S protein, followed by HRP-conjugated goat anti-mouse IgG (Jackson ImmunoResearch, West Grove, PA) at a 1:5,000 dilution. The bands detected by antibodies were visualized with chemiluminescence reagent plus (Perkin-Elmer, Boston, MA) according to the manufacturer's instructions.

**Virus neutralization assay.** To assess the ability of mouse MAbs to HKU1 S to neutralize the infectivity of HKU1 virus, the MAbs were incu-

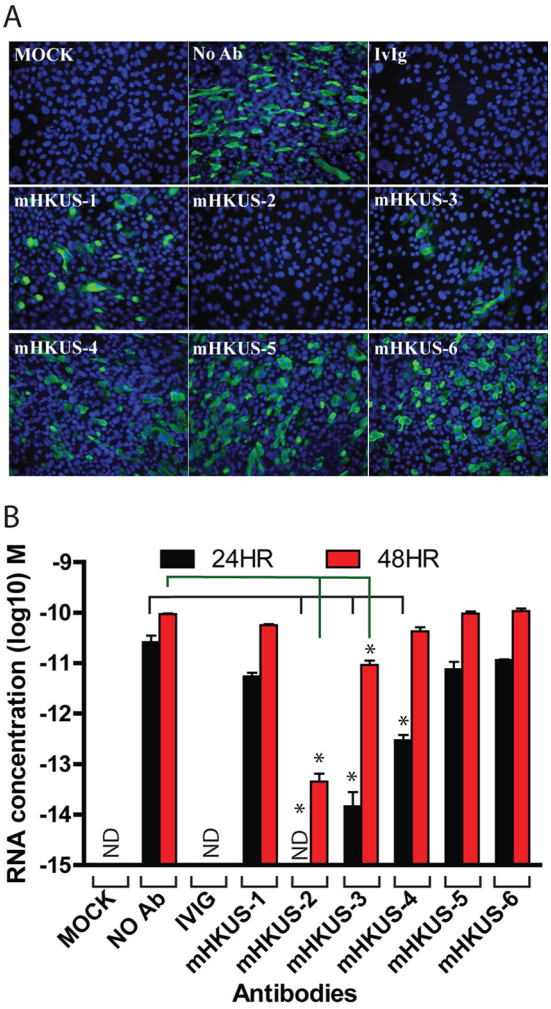


**FIG 2** Inhibition of HKU1 virus entry by mouse MAbs to HKU1 S protein. The HKU1 virus was incubated with either human IvIg (10 mg/ml) or undiluted hybridoma supernatants of the indicated mouse MAbs for 30 min at 37°C, and then virus-antibody mixtures were incubated on apical surfaces of differentiated HTBE cells for 4 h. After removing the inocula, cells were washed and then incubated for another 48 h. Infected cells were detected by IFA with polyclonal rabbit 1814 anti-HKU1 S antibody (A), and RNA from released viruses from apical washes at 24 and 48 h postinoculation were analyzed by real-time PCR (B). No Ab, 1% BSA but no antibody; IvIg, human IvIg at 10 mg/ml; mHKUS-1 to mHKUS-6, hybridoma supernatant antibody. ND, not detected. *, $P < 0.05$. Experiments were done at least twice; one representative is shown.

bated with a 1:100 dilution of passage 1 or passage 3 of HKU1 virus for 30 min at 34°C, and then the virus-antibody mixtures were inoculated onto the apical surface of differentiated HTBE cells and incubated for 4 h at 34°C. After removal of the virus-antibody mixture, the apical surfaces of the cells were washed twice with DMEM plus 1% BSA to remove unbound virus, followed by a third wash with 150 μl of DMEM plus 1% BSA that was collected for RT-PCR analysis at the 4-h time point. Cells again were washed once with 150 μl of DMEM plus 1% BSA at 24 h and 48 h postinoculation. Cells were fixed at 48 h postinoculation and assayed for HKU1 infection by IFA using rabbit 1814 polyclonal anti-HKU1 S antibodies.

**Blockade of HKU1 virus entry by preincubation with soluble HKU1 S proteins.** Differentiated HTBE cells were incubated with various amounts of soluble, truncated HKU1 S proteins for 1 h at 37°C. Passage 1

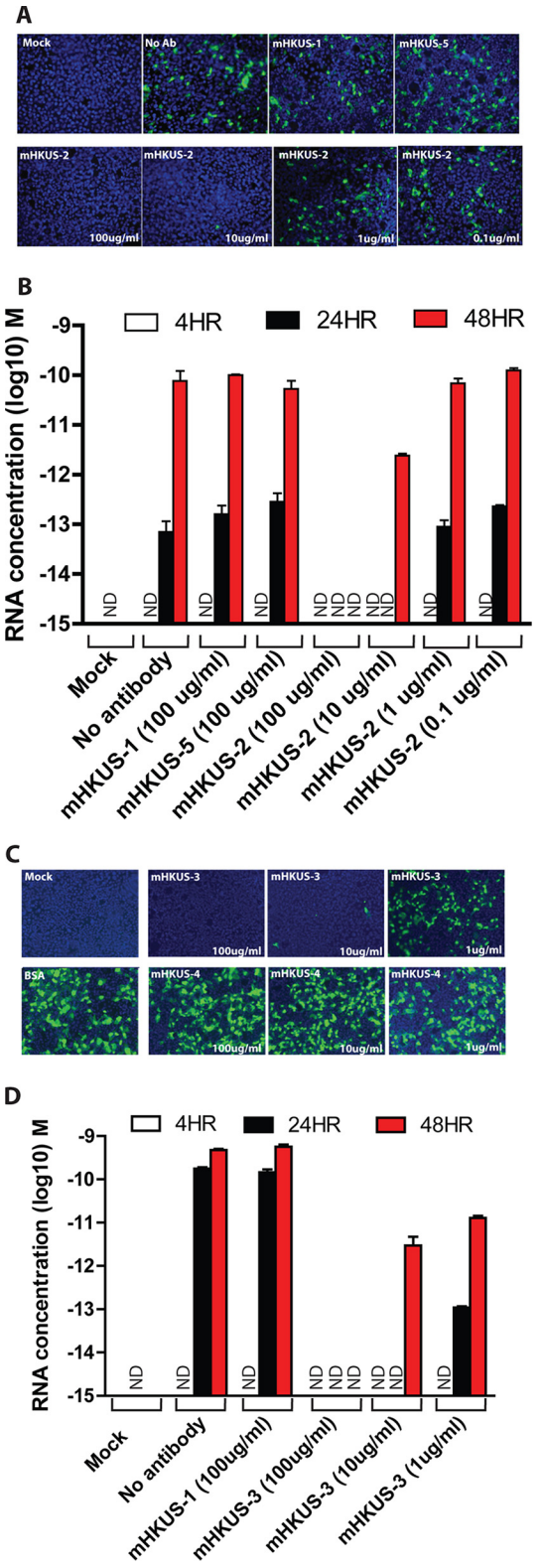


**FIG 3** Dose-dependent inhibition of HKU1 virus entry by antibodies mHKUS-2 and mHKUS-3. Inhibition experiments were performed as described for Fig. 2 using the given amount of purified antibodies. (A and C) IFA; (B and D) real-time PCR analysis. (A and B) Viruses from passage 1; (C and D) viruses from passage 3. No antibody, 1% BSA but no antibody. mHKUS-1 and mHKUS-5 served as negative controls at concentrations of 100 μg/ml. Experiments were repeated at least twice, and one representative is shown. ND, not detected.

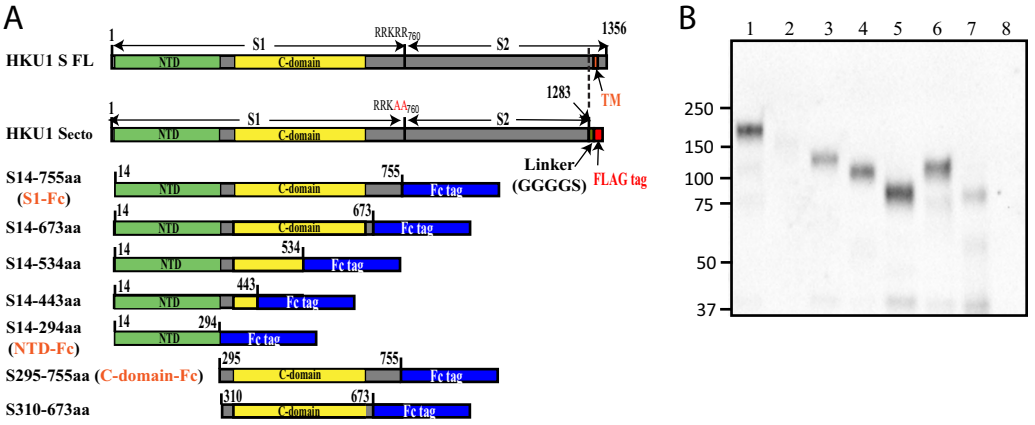


**FIG 4** Western blot analysis of N-, C-, or both terminal truncations of HKU1 S proteins. (A) Schematic diagram of N-, C-, or both terminal truncations of HKU1 S proteins. The truncated proteins with C-terminal Fc tags were purified and detected by HRP-conjugated goat anti-human IgG. The amino acid positions are indicated relative to those of wild-type HKU1 S protein. NTD, N-terminal domain; CTD, C-terminal domain; TM, transmembrane domain; linker GGGGS, flexible linker gly-gly-gly-gly-ser; FLAG tag, DYKDDDDK. (B) Western blot analysis of truncated HKU1 S protein expression. Truncated protein was separated in a 4 to 15% SDS-PAGE and transferred to nitrocellulose membranes. The blots were probed with HRP-conjugated goat anti-human IgG antibody. Lane 1, S14-755; lane 2, S14-673; lane 3, S14-534; lane 4, S14-443; lane 5, S14-294; lane 6, S295-755; lane 7, S310-673; lane 8, mock-transfected control. Lanes 1 to 6 were blotted with undiluted hybridoma supernatants (Sups), and lane 7 was blotted with a 10-fold concentrated hybridoma supernatant. Experiments were done three times, and one representative is shown.

amplified HKU1 virus then was diluted into an equal volume of each HKU1 S protein and inoculated onto the apical surface of HTBE cells. After 4 h of incubation at 34°C, the virus-protein mixture was removed and cells were washed twice with DMEM plus 1% BSA, followed by a third wash with 150 μl of DMEM plus 1% BSA that was collected for RT-PCR analysis of viral RNA in released virus at the 4-h time point. Cells again were washed once with 150 μl of DMEM plus 1% BSA at 24 h and 48 h postinoculation, fixed at 48 h postinoculation, and assayed for infection by immunofluorescence as described above.

## RESULTS

**Characterization of MAbs to HKU1 S protein antibodies.** We generated a panel of mouse monoclonal antibodies (MAbs) to purified, soluble trimeric FLAG-tagged HKU1-$S_{ecto}$ protein. Six MAbs, called mHKUS-1, mHKUS-2, mHKUS-3, mHKUS-4, mHKUS-5, and mHKUS-6, with high affinity to purified HKU1-$S_{ecto}$ in ELISA, were selected for further study by immunofluorescence assay (IFA) and Western blot analysis. As shown in Fig. 1A and Table 1, 293T cells transiently expressing HKU1 S protein and fixed with methanol were strongly recognized by IFA with MAbs mHKUS-1 and mHKUS-4. In contrast, mHKUS-2, mHKUS-3, mHKUS-5, and mHKUS-6 bound less strongly to cells expressing S protein (Fig. 1A and Table 1). None of the six selected anti-HKU1-S MAbs cross-reacted with any of the S proteins from β-CoVs mouse hepatitis virus (MHV), bovine coronavirus (BCoV), SARS-CoV, or MERS-CoV or from the human α-CoVs 229E and NL63 (Table 1).

We next tested whether any of the 6 MAbs could recognize purified, truncated, and denatured HKU1 S proteins by Western blotting. The mHKUS-1 antibody bound strongly to purified S14-294aa by Western blotting and bound very weakly, but consistently slightly above background levels, to S295-755aa (Fig. 1B). None of the 5 other MAbs showed any significant level of binding to truncated HKU1 S proteins or S proteins of other CoVs by Western blotting (Fig. 1B and data not shown).

**Effects of monoclonal antibodies on virus entry and release.** We next evaluated whether any of the 6 MAbs to HKU1 S protein were able to inhibit entry of HKU1 virus into HTBE cells. As we previously showed (36), human intravenous immunoglobulin (IvIg) at 10 mg/ml effectively neutralized the infectivity of HKU1 virus from a clinical isolate and prevented infection of primary, differentiated HTBE cells (Fig. 2A and B), indicating that pooled human sera contain antibodies that can neutralize HKU1. Incubation of HKU1 virus with hybridoma supernatant containing mHKUS-2 strongly neutralized HKU1 virus infection of HTBE cells, and mHKUS-3 antibody also reduced HKU1 virus entry (Fig. 2A). None of the 4 other HKU1 S MAbs had virus neutralizing activity detected using IFA.

To further evaluate the effect of the MAbs on HKU1 virus entry and infection, we also used real-time PCR to quantitate the yield of viral RNA from virions released from HTBE cells inoculated with MAb-virus mixtures. Released virus in apical washes was collected at 24 and 48 hpi, and viral RNA was extracted and quantitated by real-time PCR. Figure 2B shows that mHKUS-2 antibody reduced the yield of RNA from virus released from HTBE cells by over 20,000-fold and over 2,000-fold relative to the no-MAb control at 24 and 48 hpi, respectively. By 24 hpi, supernatant containing mHKUS-3 had reduced virus release by over 1,700-fold, but by 48 hpi, virus RNA in supernatant had increased significantly and was only about 10-fold less than that of the no-antibody control. The mHKUS-4 antibody caused an over 80-fold reduction on virus RNA release at 24 hpi but had no effect on virus RNA release by 48 hpi. Thus, although neutralization of HKU1 virus infectivity by MAbs mHKUS-2, -3, and -4 was detectable at 24 h, apparently small amounts of virus that escaped neutralization were able to catch up and spread through the cultures by 48 h, most likely because the continuous presence of inhibitory antibody could not be sustained on the apical cell membrane, as it was maintained at an air-liquid interface. The MAbs mHKUS-1, -5, and -6 showed no virus neutralization activity at 24 or 48 hpi (Fig. 2B).

To further evaluate the virus-neutralizing activities of MAbs mHKUS-2, -3, and -4, we used purified mHKUS-2, -3, and -4 MAbs to determine the concentration of antibodies required for

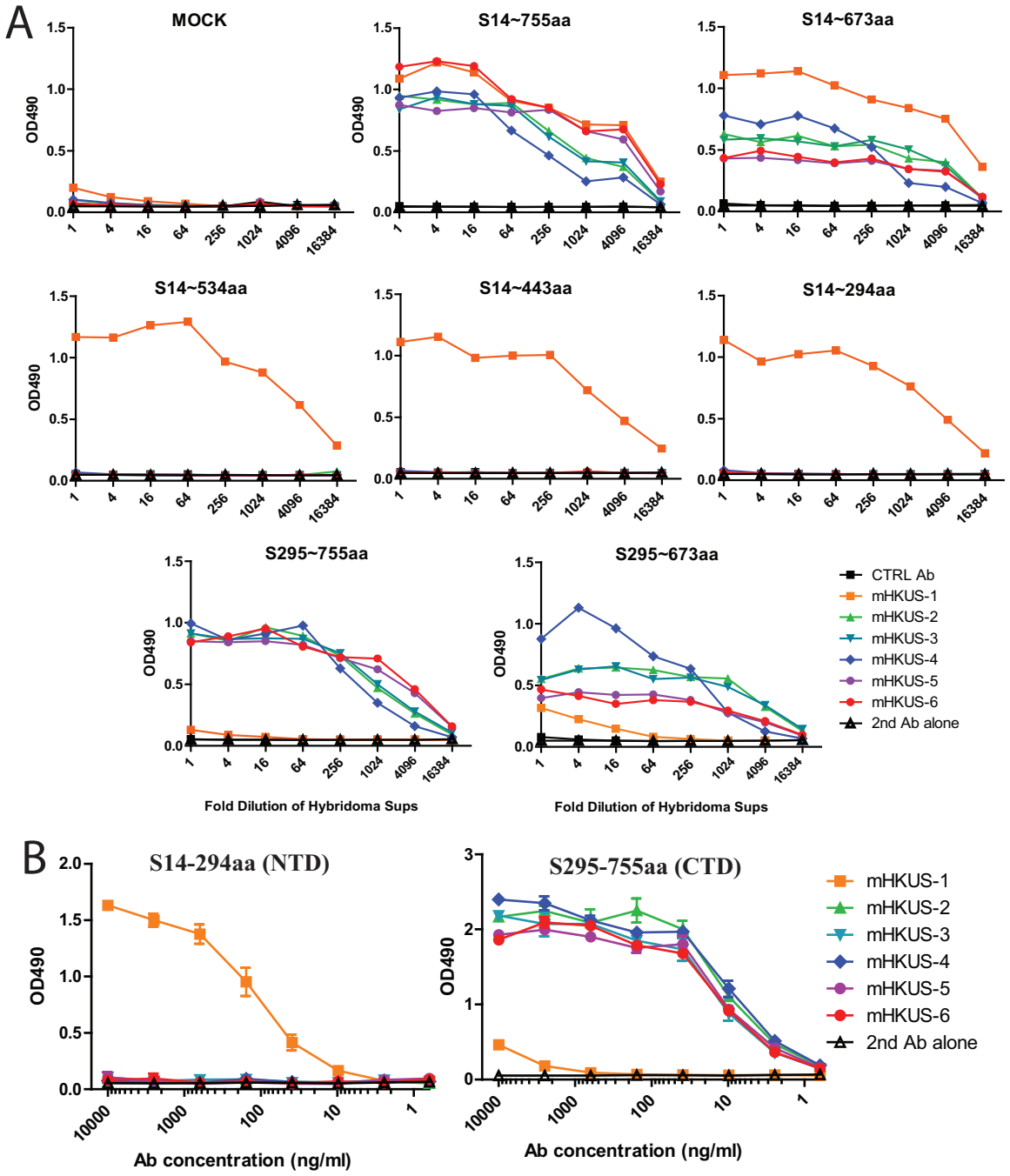


**FIG 5** Mapping of epitopes of MAbs to HKU1 S protein. (A) ELISAs were performed using supernatant containing the indicated proteins. Ctrl Ab, negative-control antibody; 2nd Ab control, no primary antibody but with 2nd Ab. Experiments were done twice, and one representative is shown. (B) ELISAs were performed using purified proteins and purified antibodies. The experiments were done twice, and one representative is shown.

effective inhibition of virus entry. Purified mHKUS-1 and mHKUS-5 antibodies at 100 μg/ml and mHKUS-4 antibody at 1 μg/ml, 10 μg/ml, and 100 μg/ml did not block HKU1 virus entry and production compared to the no-antibody control (Fig. 3A and C). In contrast, HKU1 virus was completely neutralized by mHKUS-2 and mHKUS-3 antibodies at a concentration of 100 μg/ml (Fig. 3A and C), and virus RNA release at 24 h and 48 h pi was below the level of detection (Fig. 3B and D). When the antibody concentration of mHKUS-2 and mHKUS-3 was reduced to 10 μg/ml, a few sporadic infected cells were observed by IFA at 48 hpi (Fig. 3A), and at 24 hpi virus RNA release was below the limit of detection. However, mHKUS-2 antibody concentrations of 1 μg/ml and 0.1 μg/ml did not significantly reduce virus entry or release of viral RNA (Fig. 3A and B), whereas mHKUS-3 antibody at a concentration of 1 μg/ml markedly reduced the release of viral RNA (Fig. 3C and D). These results indicate that antibody mHKUS-2 at a concentration of 10 μg/ml, but not at 1 μg/ml, can effectively neutralize HKU1 virus and block virus entry and release

of virions, whereas antibody mHKUS-3 can effectively neutralize HKU1 virus at a concentration of 1 μg/ml.

**Mapping the location of the neutralization epitopes of mHKUS-2 and mHKUS-3 MAbs.** To determine where on HKU1 S protein the epitopes recognized by neutralizing MAbs mHKUS-2 and mHKUS-3 are located, we engineered a series of plasmids that encode soluble, human Fc-tagged HKU1 S proteins with either N-terminal truncation (S295-755aa), C-terminal truncations (S14-755aa, S14-673aa, S14-534aa, S14-443aa, or S14-294aa), or both N- and C-terminal truncations (S310-673aa) (Fig. 4A). The sites selected for these N-terminal or C-terminal truncations were selected based on the alignment of HKU1 S protein with other CoV S proteins with known receptor-binding domains. All but two of the truncated HKU1 S proteins were expressed well in 293T cells (Fig. 4B). The S14-673aa and the S310-673aa proteins were considerably less stable than the other truncated S proteins, so it was necessary to use 10-fold-concentrated supernatants for Western blot and ELISA analysis (Fig. 4B).

Although all of the MAbs to HKU1 S recognized the full-length HKU1 S1 domain (S14-755aa) and the nearly full-length S1 domain, S14-673aa, in ELISA (Fig. 5), several MAbs behaved slightly differently. For example, although mHKUS-1 and mHKUS-6 bound similarly to S14-755, antibody mHKUS-1 bound to S14-673aa protein significantly better than mHKUS-6 (Fig. 5A). These data suggest that the epitope recognized in S14-673aa has a slightly different conformation than that in S14-755aa.

Only MAb mHKUS-1 bound to S14-534aa, suggesting that the epitopes for antibodies mHKUS-2 through mHKUS-6 are located between amino acids 535 and 673 of HKU1 S protein and that the mHKUS-1 epitope likely lies between S14-534aa (Fig. 5A). To further delineate the epitope recognized by MAb mHKUS-1, we tested its ability to recognize the smaller S14-443aa and S14-294aa truncated S proteins and found that MAb mHKUS-1 bound to both. Therefore, the epitope recognized by mHKUS-1 likely is located within S14-294aa, which contains the N-terminal domain (NTD) of β-CoVs (Fig. 5A). In support of this conclusion, mHKUS-1 showed minimal binding to S295-673aa and S295-755aa (Fig. 5A).

To compare the binding affinities of the MAbs to HKU1 S proteins, we performed ELISAs using purified S14-294aa and S295-755aa proteins with purified MAbs. Figure 5B shows that only mHKUS-1 antibody recognized S14-294aa protein. Binding of MAb mHKUS-1 to S14-294aa was detected at 10 ng/ml, and signal gradually increased as antibody concentration increased, plateauing at around 10 μg/ml. While mHKUS-2, -3, -4, -5, and -6 MAbs did not bind to S14-294aa protein, all recognized the S295-755aa protein and their binding patterns were very similar, with binding detectable at 2.5 ng/ml and reaching a plateau at 40 ng/ml.

**Receptor blockade of HKU1 virus infection by truncated S proteins.** Since the epitopes of MAbs mHKUS-2 and mHKUS-3, the HKU1 virus-neutralizing MAbs, mapped between amino acids 535 and 673, we reasoned that this most likely is part of the receptor-binding domain (RBD) located within the C domain (S295-755aa) of the HKU1 S protein. To test this hypothesis, S14-755aa-Fc (S1), S14-294aa-Fc (NTD), and S295-755aa-Fc (C domain) proteins were purified and preincubated with HTBE cells to occupy the virus receptor on the cell surface. Because of its poor stability, we did not test the S310-673aa protein. Preincubation of HTBE cells with S1-Fc protein at 2.5 μM significantly blocked HKU1 virus entry (Fig. 6A) and reduced virus release from cells by

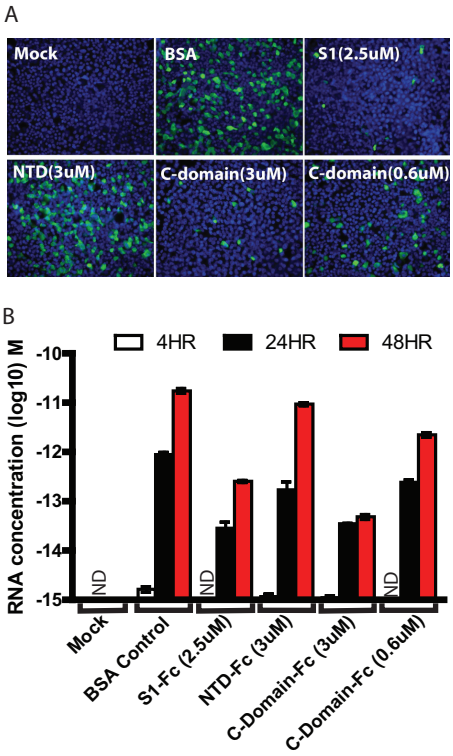


**FIG 6** Inhibition of HKU1 virus entry by CTD of HKU1 S protein. Differentiated HTBE cells were incubated with the indicated amount of S1, NTD, or CTD proteins at 37°C for 1 h. HKU1 viruses were diluted into the same amount of proteins and added onto the HTBE cells for 4 h. After being washed, cells were fixed and stained with polyclonal rabbit anti-HKU1 S antibodies at 48 h postinoculation (A), and released viruses from apical washes at 4 h, 24, and 48 h of postinoculation were analyzed by real-time PCR (B). ND, not detected.

31-fold at 24 hpi (Fig. 6B). However, preincubation of the cells with purified NTD-Fc protein at 3 μM did not significantly reduce the number of cells infected by HKU1 virus compared to that of the BSA control by IFA (Fig. 6A). In contrast, preincubation of HTBE cells with the purified C domain-Fc at 3 μM markedly decreased HKU1 virus infection by IFA (Fig. 6A) and reduced virus release by 25-fold and 360-fold at 24 and 48 h postinoculation, respectively, compared to that of the BSA controls (Fig. 6B). The inhibition effect by C domain protein was dose dependent, since C domain-Fc at 0.6 μM also showed an inhibitory effect on HKU1 virus entry (Fig. 6B). These results, together with the mapping of the virus-neutralizing MAbs to the C domain, strongly suggest that the HKU1 RBD is located within the C domain of the HKU1 S protein, likely between amino acids 535 and 673.

## DISCUSSION

Membrane fusion mediated by class I viral fusion proteins is the complex process involving transition from the metastable prefusion state to the six-helix bundle postfusion state. The receptor binding and/or pH change act to trigger this cascade. Most coronaviruses use the C domains of their S proteins to bind to their respective receptors and trigger this fusion (Fig. 7). All of the known RBDs of α-CoVs are located within the C domain, although NTDs of S protein of some α-CoVs bind sugar (Fig. 7A). The RBDs of SARS-CoV, a group B β-CoV, and MERS CoV, a


**FIG 7** Coronavirus spike proteins. (A) Diagram of coronavirus spike proteins. NTD, N-terminal domain; HRN, N-terminal heptad repeat; HRC, C-terminal heptad repeat. Group indicates the CoV genus and group. (B) Amino acid sequence alignment of S1 subunits of different betacoronaviruses. The letters with red underlining and red arrows are the contacting residues of MHV S protein with mouse CEACAM1a, while the letters with black underlining and black arrows are the sugar binding residues of BCoV S protein. The similarity of S1 among group A betacoronaviruses is about 71.9%, whereas the similarity of S1 among different group betacoronaviruses is about 29.4%.

group C β-CoV, also are located within the C domain (20, 21, 42). In contrast, all known β-CoVs in group A use their NTDs to bind protein receptors or sugars (Fig. 7) (43, 44). Despite the fact that the MHV NTD folds like a galectin, it has evolved to bind mCEACAM1a. Although their protein receptor remains to be determined, the galectin-like fold NTDs of BCoV and OC43 bind to 9-*O*-acetyl sialic acid, which is essential for virus attachment (27, 45).

Surprisingly, we found that HKU1 virus, another β-CoV in group A, uses its C domain, not NTD, to engage with its yet-to-be-identified receptor. To our knowledge, this is the first study demonstrating that the RBD of the HKU1 S protein is located within the C domain. Truncated HKU1 S protein with the C domain, not NTD, effectively reduced HKU1 virus infection on HTBE cells. Despite the fact that the NTD of group A β-CoV HKU1 is highly homologous to the NTDs of MHV, OC43, and BCoV, its biological activity appears to be strikingly different from that of the NTDs of these related viruses. The purified HKU1 NTD binds to neither sugar (43) nor human carcinoembryonic antigen-related cell adhesion molecules (CEACAMs) (data not shown), and the NTD does not inhibit HKU1 virus entry (Fig. 6). Failure of HKU1 NTD to bind a sugar or protein receptor is particular intriguing, since several critical sugar-interacting residues (Y162, E182, W184, and H185) in BCoV's NTD are conserved in HKU1's NTD (Fig. 7B) (44). In addition, the NTD of MHV binding to mCEACAM1a is necessary and sufficient for membrane fusion (19, 43, 46, 47), indicating that the binding of receptor by the NTD of a group A β-CoV can trigger the membrane fusion cascade. Thus, two β-CoVs in group A, HKU1 and MHV, have evolved to use different regions of their spike glycoproteins to recognize their respective receptor proteins and trigger the conformational changes of S protein leading to membrane fusion. This is a new example of the modular nature of the spike proteins of CoVs (29, 48), in which binding and entry of two CoVs in the same group are initiated by different regions of the spike glycoprotein. The exact mechanism of how these two different domains trigger the membrane fusion requires further investigation.

Interestingly, five of the six monoclonal antibodies bound the C domain, while only one, mHKUS-1, recognized the NTD. These results indicate that the C domain is highly immunogenic. Further epitope mapping revealed that the epitopes of all five C domain antibodies are located within amino acids 535 to 673 (Fig. 5), suggesting that this region is immunodominant. We also found that two of these antibodies were able to inhibit infection of HKU1 viruses, effectively indicating that this region (aa 535 to 673) contains neutralizing epitopes. Within certain domains, the HKU1 spike glycoprotein displays remarkable sequence homology to other betacoronaviruses (Fig. 7B). Of note, within our mapped neutralizing HKU1 spike epitope (aa 535 to 673), amino acid sequences of 535 to 551, 573 to 583, 587 to 609, and 613 to 673 of HKU1 S protein are almost identical to either BCoV or MHV S protein. Since none of our HKU1 antibodies cross-reacted with MHV or BCoV S proteins (Table 1), the neutralizing HKU1 epitope likely lies in the highly diverse region encompassing amino acids 552 to 572, 584 to 586, and/or 610 to 612. For many enveloped viruses, highly immunogenic neutralization epitopes often are located in or around the viral RBD (49–51). Therefore, we propose that amino acids 535 to 673, and possibly amino acids 552 to 572, 584 to 586, and 610 to 612, of the HKU1 spike protein contain the RBD. Of note, the receptor-binding motifs of many viral spike proteins are comprised of residues that are spatially close but largely separated in primary sequence (20, 21). Our neutralizing antibodies, mHKUS-2 and mHKUS-3, do not recognize denatured C domain truncated S protein well, indicating that the neutralizing epitope is conformation dependent. Thus, the RBD of HKU1 S protein may contain residues outside this proposed region, potentially within the highly variable regions encompassing amino acids 451 to 457, 463 to 472, 477 to 494, 502 to 521, and/or 527 to 532.

Phylogenetically, there are three genotypes of HKU1 viruses (A, B, and C) resulting from viral recombination events (52). Although S proteins from these genotypes are highly conserved, there are noticeable differences between genotype A and genotype B or C, which are identical. In particular, the sequences encompassing amino acid 558 and 568 (amino acid numbering from HKU1 S protein clade A) of S proteins are markedly different between genotypes A and B/C. Because of these differences, it will be important to determine whether our neutralizing antibodies also neutralize HKU1 viruses from genotype B/C and whether any of our monoclonal antibodies can differentiate these genotypes in IFA and ELISA for diagnostic purposes. Unfortunately, lack of genotype B or C isolates hindered our ability to investigate these differences.

In summary, using a panel of HKU1 S protein-specific MAbs, we identified the C domain as the locus of epitopes recognized by two HKU1 neutralizing MAbs and showed that the soluble C domain can induce receptor blockade resulting in inhibition of HKU1 infection. These data demonstrate that the RBD of HKU1 is located within the C domain of the S protein, likely between amino acids 547 and 573. These results highlight that several β-CoVs in group A have evolved to use different regions of their spike glycoproteins to recognize their respective receptors. These findings will aid studies of HKU1 virus pathogenesis and receptor discovery and facilitate development of new models for β-CoV evolution.

## ACKNOWLEDGMENTS

This work was supported by grant 5K08-A1073525 from the National Institute of Allergy and Infectious Diseases, NIH, USA, to S.R.D. and grants from the Chinese Science and Technology Key Projects (2014ZX10004001), National Natural Science Foundation of China (31470266), and Institute of Pathogen Biology, CAMS (2014IPB101), to Z.Q. This work was also supported by the PUMC Youth Fund, Fundamental Research Funds for the Central Universities (3332013118), and the Program for Changjiang Scholars and Innovative Research Team in University (IRT13007). The monoclonal antibodies were prepared by the Protein Production Shared Resource of the University of Colorado School of Medicine, Aurora, Colorado, which is supported by the National Cancer Institute, NIH, USA, through a cancer center support grant (P30CA046934).

## REFERENCES

1. **Masters PS, Perlman S.** 2013. Coronaviridae, p 825–858. *In* Knipe DM, Howley PM, Cohen JI, Griffin DE, Lamb RA, Martin MA, Racaniello VR, Roizman B (ed), Fields virology, 6th ed. Lippincott Williams & Wilkins, Philadelphia, PA.
2. **de Groot RJ, Baker SC, Baric RS, Brown CS, Drosten C, Enjuanes L, Fouchier RA, Galiano M, Gorbalenya AE, Memish ZA, Perlman S, Poon LL, Snijder EJ, Stephens GM, Woo PC, Zaki AM, Zambon M, Ziebuhr J.** 2013. Middle East respiratory syndrome coronavirus (MERS-CoV): announcement of the Coronavirus Study Group. J Virol **87:**7790–7792. http://dx.doi.org/10.1128/JVI.01244-13.
3. **Graham RL, Donaldson EF, Baric RS.** 2013. A decade after SARS: strat-

egies for controlling emerging coronaviruses. Nat Rev Microbiol **11:**836–848. http://dx.doi.org/10.1038/nrmicro3143.

4. **King AMQ, Adams MJ, Carstens EB, Lefkowitz EJ (ed).** 2011. Virus taxonomy: classification and nomenclature of viruses. Ninth report of the International Committee on Taxonomy of Viruses. Academic Press, London, United Kingdom.
5. **Drosten C, Gunther S, Preiser W, van der Werf S, Brodt HR, Becker S, Rabenau H, Panning M, Kolesnikova L, Fouchier RA, Berger A, Burguiere AM, Cinatl J, Eickmann M, Escriou N, Grywna K, Kramme S, Manuguerra JC, Muller S, Rickerts V, Sturmer M, Vieth S, Klenk HD, Osterhaus AD, Schmitz H, Doerr HW.** 2003. Identification of a novel coronavirus in patients with severe acute respiratory syndrome. N Engl J Med **348:**1967–1976. http://dx.doi.org/10.1056/NEJMoa030747.
6. **Hamre D, Procknow JJ.** 1966. A new virus isolated from the human respiratory tract. Proc Soc Exp Biol Med **121:**190–193. http://dx.doi.org/10.3181/00379727-121-30734.
7. **Ksiazek TG, Erdman D, Goldsmith CS, Zaki SR, Peret T, Emery S, Tong S, Urbani C, Comer JA, Lim W, Rollin PE, Dowell SF, Ling AE, Humphrey CD, Shieh WJ, Guarner J, Paddock CD, Rota P, Fields B, DeRisi J, Yang JY, Cox N, Hughes JM, LeDuc JW, Bellini WJ, Anderson LJ.** 2003. A novel coronavirus associated with severe acute respiratory syndrome. N Engl J Med **348:**1953–1966. http://dx.doi.org/10.1056/NEJMoa030781.
8. **McIntosh K, Becker WB, Chanock RM.** 1967. Growth in suckling-mouse brain of "IBV-like" viruses from patients with upper respiratory tract disease. Proc Natl Acad Sci U S A **58:**2268–2273. http://dx.doi.org/10.1073/pnas.58.6.2268.
9. **Peiris JS, Lai ST, Poon LL, Guan Y, Yam LY, Lim W, Nicholls J, Yee WK, Yan WW, Cheung MT, Cheng VC, Chan KH, Tsang DN, Yung RW, Ng TK, Yuen KY.** 2003. Coronavirus as a possible cause of severe acute respiratory syndrome. Lancet **361:**1319–1325. http://dx.doi.org/10.1016/S0140-6736(03)13077-2.
10. **van der Hoek L, Pyrc K, Jebbink MF, Vermeulen-Oost W, Berkhout RJ, Wolthers KC, Wertheim-van Dillen PM, Kaandorp J, Spaargaren J, Berkhout B.** 2004. Identification of a new human coronavirus. Nat Med **10:**368–373. http://dx.doi.org/10.1038/nm1024.
11. **Woo PC, Lau SK, Chu CM, Chan KH, Tsoi HW, Huang Y, Wong BH, Poon RW, Cai JJ, Luk WK, Poon LL, Wong SS, Guan Y, Peiris JS, Yuen KY.** 2005. Characterization and complete genome sequence of a novel coronavirus, coronavirus HKU1, from patients with pneumonia. J Virol **79:**884–895. http://dx.doi.org/10.1128/JVI.79.2.884-895.2005.
12. **Zaki AM, van Boheemen S, Bestebroer TM, Osterhaus AD, Fouchier RA.** 2012. Isolation of a novel coronavirus from a man with pneumonia in Saudi Arabia. N Engl J Med **367:**1814–1820. http://dx.doi.org/10.1056/NEJMoa1211721.
13. **Lee N, Hui D, Wu A, Chan P, Cameron P, Joynt GM, Ahuja A, Yung MY, Leung CB, To KF, Lui SF, Szeto CC, Chung S, Sung JJ.** 2003. A major outbreak of severe acute respiratory syndrome in Hong Kong. N Engl J Med **348:**1986–1994. http://dx.doi.org/10.1056/NEJMoa030685.
14. **White JM, Delos SE, Brecher M, Schornberg K.** 2008. Structures and mechanisms of viral membrane fusion proteins: multiple variations on a common theme. Crit Rev Biochem Mol Biol **43:**189–219. http://dx.doi.org/10.1080/10409230802058320.
15. **Bonavia A, Zelus BD, Wentworth DE, Talbot PJ, Holmes KV.** 2003. Identification of a receptor-binding domain of the spike glycoprotein of human coronavirus HCoV-229E. J Virol **77:**2530–2538. http://dx.doi.org/10.1128/JVI.77.4.2530-2538.2003.
16. **Du L, Zhao G, Kou Z, Ma C, Sun S, Poon VK, Lu L, Wang L, Debnath AK, Zheng BJ, Zhou Y, Jiang S.** 2013. Identification of a receptor-binding domain in the S protein of the novel human coronavirus Middle East respiratory syndrome coronavirus as an essential target for vaccine development. J Virol **87:**9939–9942. http://dx.doi.org/10.1128/JVI.01048-13.
17. **Godet M, Grosclaude J, Delmas B, Laude H.** 1994. Major receptor-binding and neutralization determinants are located within the same domain of the transmissible gastroenteritis virus (coronavirus) spike protein. J Virol **68:**8008–8016.
18. **Hofmann H, Simmons G, Rennekamp AJ, Chaipan C, Gramberg T, Heck E, Geier M, Wegele A, Marzi A, Bates P, Pohlmann S.** 2006. Highly conserved regions within the spike proteins of human coronaviruses 229E and NL63 determine recognition of their respective cellular receptors. J Virol **80:**8639–8652. http://dx.doi.org/10.1128/JVI.00560-06.
19. **Kubo H, Yamada YK, Taguchi F.** 1994. Localization of neutralizing epitopes and the receptor-binding site within the amino-terminal 330 amino acids of the murine coronavirus spike protein. J Virol **68:**5403–5410.
20. **Li F, Li W, Farzan M, Harrison SC.** 2005. Structure of SARS coronavirus spike receptor-binding domain complexed with receptor. Science **309:**1864–1868. http://dx.doi.org/10.1126/science.1116480.
21. **Lu G, Hu Y, Wang Q, Qi J, Gao F, Li Y, Zhang Y, Zhang W, Yuan Y, Bao J, Zhang B, Shi Y, Yan J, Gao GF.** 2013. Molecular basis of binding between novel human coronavirus MERS-CoV and its receptor CD26. Nature **500:**227–231. http://dx.doi.org/10.1038/nature12328.
22. **Mou H, Raj VS, van Kuppeveld FJ, Rottier PJ, Haagmans BL, Bosch BJ.** 2013. The receptor binding domain of the new Middle East respiratory syndrome coronavirus maps to a 231-residue region in the spike protein that efficiently elicits neutralizing antibodies. J Virol **87:**9379–9383. http://dx.doi.org/10.1128/JVI.01277-13.
23. **Wu K, Peng G, Wilken M, Geraghty RJ, Li F.** 2012. Mechanisms of host receptor adaptation by severe acute respiratory syndrome coronavirus. J Biol Chem **287:**8904–8911. http://dx.doi.org/10.1074/jbc.M111.325803.
24. **Yang Y, Du L, Liu C, Wang L, Ma C, Tang J, Baric RS, Jiang S, Li F.** 2014. Receptor usage and cell entry of bat coronavirus HKU4 provide insight into bat-to-human transmission of MERS coronavirus. Proc Natl Acad Sci U S A **111:**12516–12521. http://dx.doi.org/10.1073/pnas.1405889111.
25. **Li F.** 2013. Receptor recognition and cross-species infections of SARS coronavirus. Antiviral Res **100:**246–254. http://dx.doi.org/10.1016/j.antiviral.2013.08.014.
26. **Schultze B, Krempl C, Ballesteros ML, Shaw L, Schauer R, Enjuanes L, Herrler G.** 1996. Transmissible gastroenteritis coronavirus, but not the related porcine respiratory coronavirus, has a sialic acid (N-glycolylneuraminic acid) binding activity. J Virol **70:**5634–5637.
27. **Vlasak R, Luytjes W, Spaan W, Palese P.** 1988. Human and bovine coronaviruses recognize sialic acid-containing receptors similar to those of influenza C viruses. Proc Natl Acad Sci U S A **85:**4526–4529. http://dx.doi.org/10.1073/pnas.85.12.4526.
28. **Promkuntod N, van Eijndhoven RE, de Vrieze G, Grone A, Verheije MH.** 2014. Mapping of the receptor-binding domain and amino acids critical for attachment in the spike protein of avian coronavirus infectious bronchitis virus. Virology **448:**26–32. http://dx.doi.org/10.1016/j.virol.2013.09.018.
29. **Li F.** 2015. Receptor recognition mechanisms of coronaviruses: a decade of structural studies. J Virol **89:**1954–1964. http://dx.doi.org/10.1128/JVI.02615-14.
30. **Dominguez SR, Robinson CC, Holmes KV.** 2009. Detection of four human coronaviruses in respiratory infections in children: a one-year study in Colorado. J Med Virol **81:**1597–1604. http://dx.doi.org/10.1002/jmv.21541.
31. **Woo PC, Lau SK, Yip CC, Huang Y, Yuen KY.** 2009. More and more coronaviruses: human coronavirus HKU1. Viruses **1:**57–71. http://dx.doi.org/10.3390/v1010057.
32. **Zhou W, Wang W, Wang H, Lu R, Tan W.** 2013. First infection by all four non-severe acute respiratory syndrome human coronaviruses takes place during childhood. BMC Infect Dis **13:**433. http://dx.doi.org/10.1186/1471-2334-13-433.
33. **Gralinski LE, Baric R.** 2015. Molecular pathology of emerging coronavirus infections. J Pathol **235:**185–195. http://dx.doi.org/10.1002/path.4454.
34. **Dijkman R, Jebbink MF, Koekkoek SM, Deijs M, Jonsdottir HR, Molenkamp R, Ieven M, Goossens H, Thiel V, van der Hoek L.** 2013. Isolation and characterization of current human coronavirus strains in primary human epithelial cell cultures reveal differences in target cell tropism. J Virol **87:**6081–6090. http://dx.doi.org/10.1128/JVI.03368-12.
35. **Dominguez SR, Shrivastava S, Berglund A, Qian Z, Goes LG, Halpin RA, Fedorova N, Ransier A, Weston PA, Durigon EL, Jerez JA, Robinson CC, Town CD, Holmes KV.** 2014. Isolation, propagation, genome analysis and epidemiology of HKU1 betacoronaviruses. J Gen Virol **95:**836–848. http://dx.doi.org/10.1099/vir.0.059832-0.
36. **Dominguez SR, Travanty EA, Qian Z, Mason RJ.** 2013. Human coronavirus HKU1 infection of primary human type II alveolar epithelial cells: cytopathic effects and innate immune response. PLoS One **8:**e70129. http://dx.doi.org/10.1371/journal.pone.0070129.
37. **Pyrc K, Sims AC, Dijkman R, Jebbink M, Long C, Deming D, Donaldson E, Vabret A, Baric R, van der Hoek L, Pickles R.** 2010. Culturing the unculturable: human coronavirus HKU1 infects, replicates, and produces progeny virions in human ciliated airway epithelial cell cultures. J Virol **84:**11255–11263. http://dx.doi.org/10.1128/JVI.00947-10.

38. **Li W, Moore MJ, Vasilieva N, Sui J, Wong SK, Berne MA, Somasundaran M, Sullivan JL, Luzuriaga K, Greenough TC, Choe H, Farzan M.** 2003. Angiotensin-converting enzyme 2 is a functional receptor for the SARS coronavirus. Nature **426:**450–454. http://dx.doi.org/10.1038/nature02145.
39. **Jeffers SA, Tusell SM, Gillim-Ross L, Hemmila EM, Achenbach JE, Babcock GJ, Thomas WD, Jr, Thackray LB, Young MD, Mason RJ, Ambrosino DM, Wentworth DE, Demartini JC, Holmes KV.** 2004. CD209L (L-SIGN) is a receptor for severe acute respiratory syndrome coronavirus. Proc Natl Acad Sci U S A **101:**15748–15753. http://dx.doi.org/10.1073/pnas.0403812101.
40. **Qian Z, Dominguez SR, Holmes KV.** 2013. Role of the spike glycoprotein of human Middle East respiratory syndrome coronavirus (MERS-CoV) in virus entry and syncytia formation. PLoS One **8:**e76469. http://dx.doi.org/10.1371/journal.pone.0076469.
41. **Kuypers J, Martin ET, Heugel J, Wright N, Morrow R, Englund JA.** 2007. Clinical disease in children associated with newly described coronavirus subtypes. Pediatrics **119:**e70–e76. http://dx.doi.org/10.1542/peds.2006-1406.
42. **Wang N, Shi X, Jiang L, Zhang S, Wang D, Tong P, Guo D, Fu L, Cui Y, Liu X, Arledge KC, Chen YH, Zhang L, Wang X.** 2013. Structure of MERS-CoV spike receptor-binding domain complexed with human receptor DPP4. Cell Res **23:**986–993. http://dx.doi.org/10.1038/cr.2013.92.
43. **Peng G, Sun D, Rajashankar KR, Qian Z, Holmes KV, Li F.** 2011. Crystal structure of mouse coronavirus receptor-binding domain complexed with its murine receptor. Proc Natl Acad Sci U S A **108:**10696–10701. http://dx.doi.org/10.1073/pnas.1104306108.
44. **Peng G, Xu L, Lin YL, Chen L, Pasquarella JR, Holmes KV, Li F.** 2012. Crystal structure of bovine coronavirus spike protein lectin domain. J Biol Chem **287:**41931–41938. http://dx.doi.org/10.1074/jbc.M112.418210.
45. **Schwegmann-Wessels C, Herrler G.** 2006. Sialic acids as receptor determinants for coronaviruses. Glycoconj J **23:**51–58. http://dx.doi.org/10.1007/s10719-006-5437-9.
46. **Dveksler GS, Pensiero MN, Cardellichio CB, Williams RK, Jiang GS, Holmes KV, Dieffenbach CW.** 1991. Cloning of the mouse hepatitis virus (MHV) receptor: expression in human and hamster cell lines confers susceptibility to MHV. J Virol **65:**6881–6891.
47. **Zelus BD, Schickli JH, Blau DM, Weiss SR, Holmes KV.** 2003. Conformational changes in the spike glycoprotein of murine coronavirus are induced at 37 degrees C either by soluble murine CEACAM1 receptors or by pH 8. J Virol **77:**830–840. http://dx.doi.org/10.1128/JVI.77.2.830-840.2003.
48. **Graham RL, Baric RS.** 2010. Recombination, reservoirs, and the modular spike: mechanisms of coronavirus cross-species transmission. J Virol **84:**3134–3146. http://dx.doi.org/10.1128/JVI.01394-09.
49. **Sattentau QJ.** 1996. Neutralization of HIV-1 by antibody. Curr Opin Immunol **8:**540–545. http://dx.doi.org/10.1016/S0952-7915(96)80044-6.
50. **Sui J, Li W, Murakami A, Tamin A, Matthews LJ, Wong SK, Moore MJ, Tallarico AS, Olurinde M, Choe H, Anderson LJ, Bellini WJ, Farzan M, Marasco WA.** 2004. Potent neutralization of severe acute respiratory syndrome (SARS) coronavirus by a human mAb to S1 protein that blocks receptor association. Proc Natl Acad Sci U S A **101:**2536–2541. http://dx.doi.org/10.1073/pnas.0307140101.
51. **Ying T, Du L, Ju TW, Prabakaran P, Lau CC, Lu L, Liu Q, Wang L, Feng Y, Wang Y, Zheng BJ, Yuen KY, Jiang S, Dimitrov DS.** 2014. Exceptionally potent neutralization of Middle East respiratory syndrome coronavirus by human monoclonal antibodies. J Virol **88:**7796–7805. http://dx.doi.org/10.1128/JVI.00912-14.
52. **Woo PC, Lau SK, Yip CC, Huang Y, Tsoi HW, Chan KH, Yuen KY.** 2006. Comparative analysis of 22 coronavirus HKU1 genomes reveals a novel genotype and evidence of natural recombination in coronavirus HKU1. J Virol **80:**7136–7145. http://dx.doi.org/10.1128/JVI.00509-06.